# Optical properties of biological aerosols
# Final technical report

**Rosalba Saija, Paolo Denti, Ferdinando Borghese**

*Università di Messina, Dipartimento di Fisica della Materia*
*e Tecnologie Fisiche Avanzate,*
*Salita Sperone, 31 — 98166 Messina, Italy*

## 1. Introduction

The study of the optical properties of biological aerosols, i.e. aerosols composed of biological spores and other organic compounds, presents unique difficulties both on the experimental and on the theoretical side. On the experimental side, we cite, as an example, the fact that all organic materials, both spores and organic compounds present a luminescence spectrum whose most carachteritic features occur in the range of wavelength in which the atmosphere is most absorbing. The presence of organic compounds, on the other hand, may come from combustion of mineral hydrocarbons. Moreover the spores of interest, such as anthrax, are often dangerous and possibly fatal to humans. For this reason special precautions must be taken in manipulating such spores.

As a result of these difficulties the essential parameters that are necessary for any reliable estimate of the optical spectra are not well known, to say the least. For instance all the information on the size and shape of the spores of antrax are contained in Fig.1 that we obtained from the scientists at CRDEC. Fig.1 shows that, on the average the spores have a length of $1.4 \pm 0.12 \, \mu$m, a
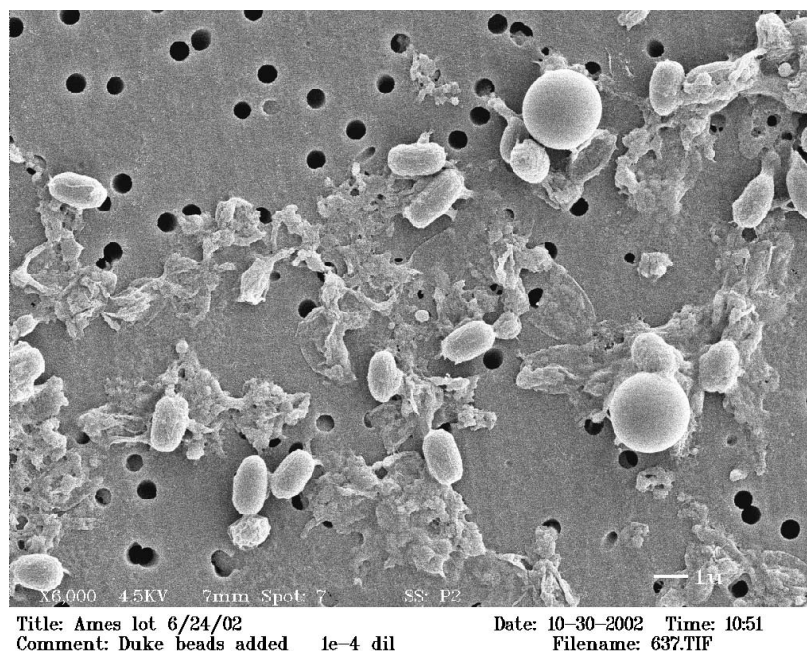


Title: Ames lot 6/24/02
Comment: Duke beads added    1e–4 dil
Date: 10–30–2002   Time: 10:51
Filename: 637.TIF

Fig. 1. Microphotograph of spores of anthrax

width of $0.82 \pm 0.05 \, \mu$m and a volume of $0.61 \pm 0.1 \, \mu$m$^3$. the diameter of the equal volume sphere is thus $1.05 \, \mu$m. The spores just described could be modelled as an aggregate of two identical,

## Report Documentation Page

| 1. REPORT DATE **2006** | 2. REPORT TYPE **N/A** | 3. DATES COVERED **-** |
|---|---|---|

| 4. TITLE AND SUBTITLE | 5a. CONTRACT NUMBER |
|---|---|
| **Optical Properties of Biological Aerosols** | 5b. GRANT NUMBER |
| | 5c. PROGRAM ELEMENT NUMBER |
| 6. AUTHOR(S) | 5d. PROJECT NUMBER |
| | 5e. TASK NUMBER |
| | 5f. WORK UNIT NUMBER |

| 7. PERFORMING ORGANIZATION NAME(S) AND ADDRESS(ES) **Universita di Messina Dipartimento di Fisica Della Materia e TEcnologie Fische Avanzate, Salita Sperone, 31 - 98166 Messina, Italy** | 8. PERFORMING ORGANIZATION REPORT NUMBER |
|---|---|
| 9. SPONSORING/MONITORING AGENCY NAME(S) AND ADDRESS(ES) | 10. SPONSOR/MONITOR'S ACRONYM(S) |
| | 11. SPONSOR/MONITOR'S REPORT NUMBER(S) |

**12. DISTRIBUTION/AVAILABILITY STATEMENT**
**Approved for public release, distribution unlimited**

**13. SUPPLEMENTARY NOTES**
**The original document contains color images.**

**14. ABSTRACT**

**15. SUBJECT TERMS**

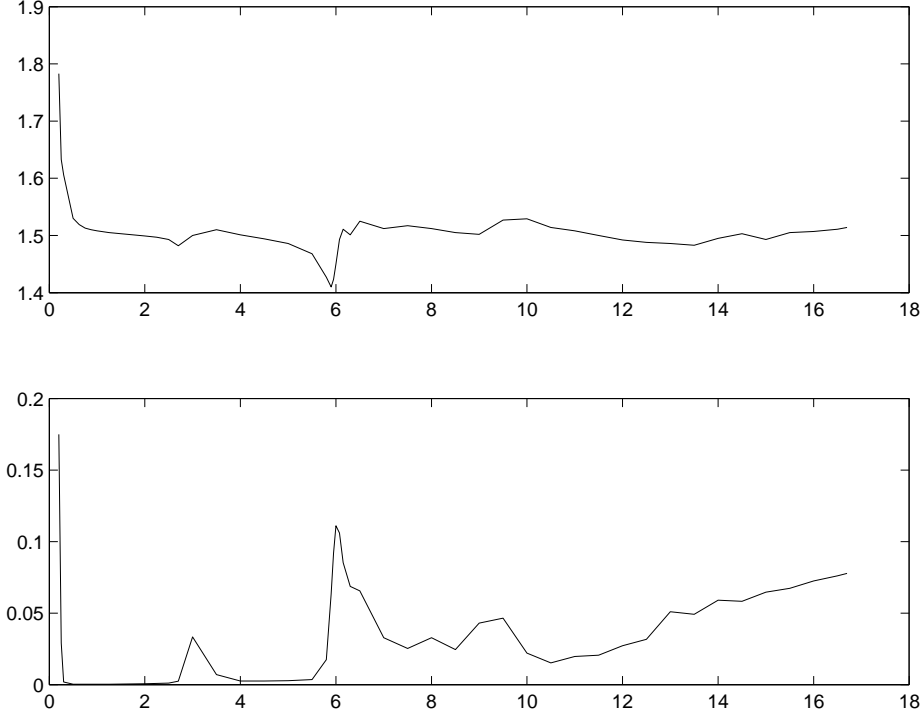| 16. SECURITY CLASSIFICATION OF: | | | 17. LIMITATION OF ABSTRACT | 18. NUMBER OF PAGES | 19a. NAME OF RESPONSIBLE PERSON |
|---|---|---|---|---|---|
| a. REPORT **unclassified** | b. ABSTRACT **unclassified** | c. THIS PAGE **unclassified** | **SAR** | **18** | |

Fig. 2. Refractive index assumed for the spores of anthrax. The upper and the lower panel report the real and the imaginary part, respectively, as a function ot the wavelength in $\mu$m.

homogeneous, mutually contacting spheres with a radius of 0.35 $\mu$m.[1] The problem lie in the lack of a reliable refractive index both of the spores as a whole and of their nucleus. We were therefore forcd to assume a wavelength-dependent refractive index whose real and imaginary parts are shown in Fig.2. Strictly speaking, the refractive index reported in Fig.2 does not belong to anthrax but to B. cereus, a spore of the same family. Nevertheless, since the refractive index of anthrax is, at the present, not known and, since B. cereus has similar optical properties, we resolved to adopt it, for the preliminary calculations that are reported in the next sections.

A further problem stems from the fact that the optical spectra recorded in the laboratory under controlled conditions come from dehydrated spores of simulants. As a result, when the spores are rehydrated, their optical properties as well as their size change so that it is important to specify the conditions under which the spores were used.[2] In fact, the critical parameters of any model used to interpretate the recorded spectra are the size and the index of refraction. We have also to mention that biological spores tend to form aggregates of comparatively big size. Therefore, as most of the calculations of the spectra of model particles are based on series expansion, the convergence of the results must be carefully checked.

All these difficulties determined the kind of research that our Group performed during the present Contract. In fact, as we stated above, a spore of anthrax can be modelled as an aggregate of two mutually contacting spheres, nevetheless an aggregate of spores turns out to be rather similar to an an aggregate of large spheres. We had thus to find general methods to check the convergence of the calculation.
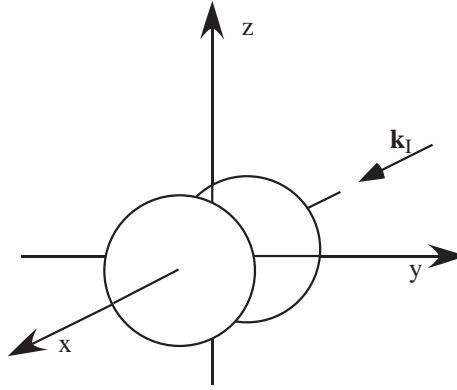
Fig. 3. Geometry adopted in our calculations. $\mathbf{k}_I$ denotes the incident wavevector.

## 2. Calculations

The technique that we used to perform our calculations is the most recent version of the theory that we developed and improved over the last twenty years and that is fully described in a recent book by the present authors.[1] In the same book the technique to calculate the scattering pattern from aggregates of spheres with a known distribution of their orientations is also described in detail. Anyway, when our calculations refer to clusters in fixed orientation, we adopted the geometry that is sketched in Fig.3, where the direction of the incident wavevector $\hat{\mathbf{k}}_I$ for head-on incidence is also drawn.

In Fig.4 (a) and (b) we report, in $\mu m^2$, the extinction and the scattering cross section for a randomly oriented dispersion of model spores. The cases of head on and of broadside incidence are also reported in Fig.4 (c) and (d) and (e) and (f), respectively. The cross sections drawn in Fig.(4) are quite regular and give a global information on the optical properties of our model. Nevertheless, a more detailed information can be gained from the 3-D graphs in Fig.(5) that report the differential scattering cross section in the forward zone, calculated at selected wavelengths. This information is rather useful in view of

the strong variability of both the real and the imaginary part of the refractive index. These plots are supplemented by the contour plots that we report in Fig.(6) that are meant to give a general idea of what pattern one should expect to see when our model spores are illuminated in fixed orientation, with the geometry described in Fig.(3). Since the geometry implies head on incidence, all the plots are independent of polarization; furthermore, all the plots show reflection symmetry around the $\theta_S$ axis. Note that in the top-left contour the wavelength is $0.25\,\mu m$ i.e. it is a little smaller than the radius of the component spheres. Therefore it is not surprising that the spherical components of the model are quite discernible. In any case all these plots should be considered as preliminary for the following reasons

- The refractive index is not the true one of the spores of anthrax but only a guess based on the similitude of B. cereus and athrax.

- The model that we adopted is a rough one and its adequacy should, therefore be further investigated so as to propose, if necessary, improved models.
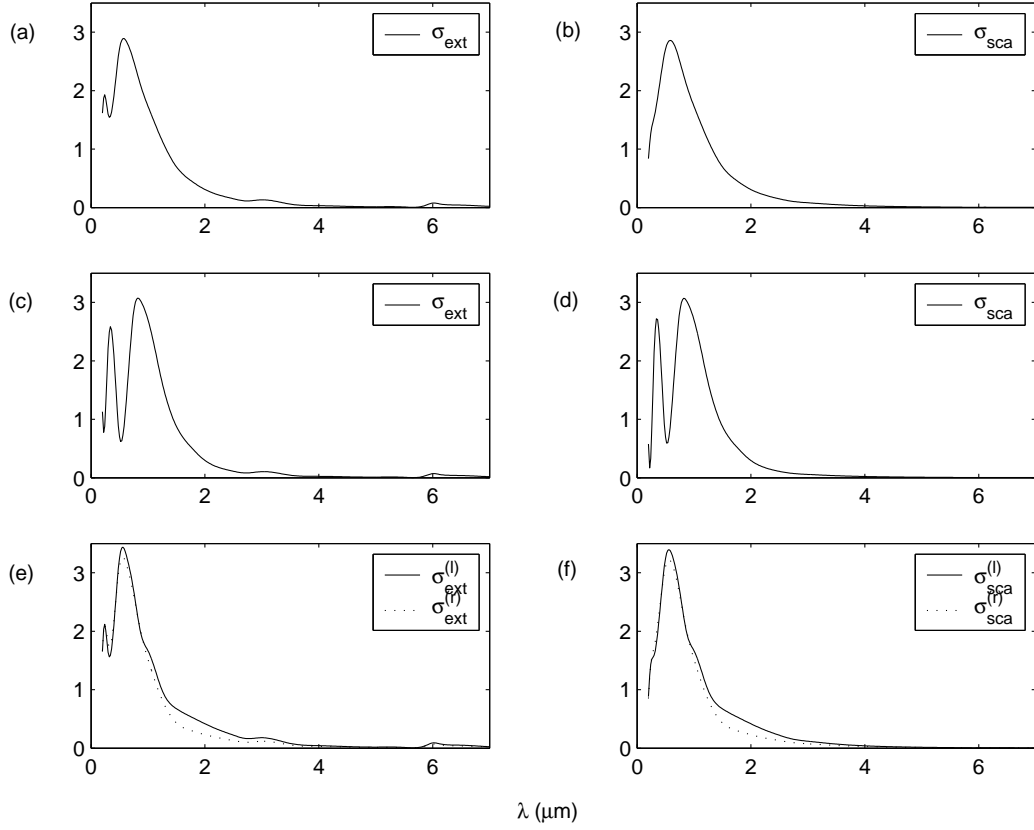
3

Fig. 4. Extinction and scattering cross section in $\mu m^2$ as a function of the wavelength in $\mu m$ for the clusters considered in the present Report. In (a) and (b) random orientation is considered; in (c) and (d) the incidence is head on; in (e) and (f) the incidence is broadside. Note that neither the case of random orientation nor the case of head on incidence depend on the polarization, as expected. The polarization dependence of the cross sections is, instead, well discernible in the case of broadside incidence.
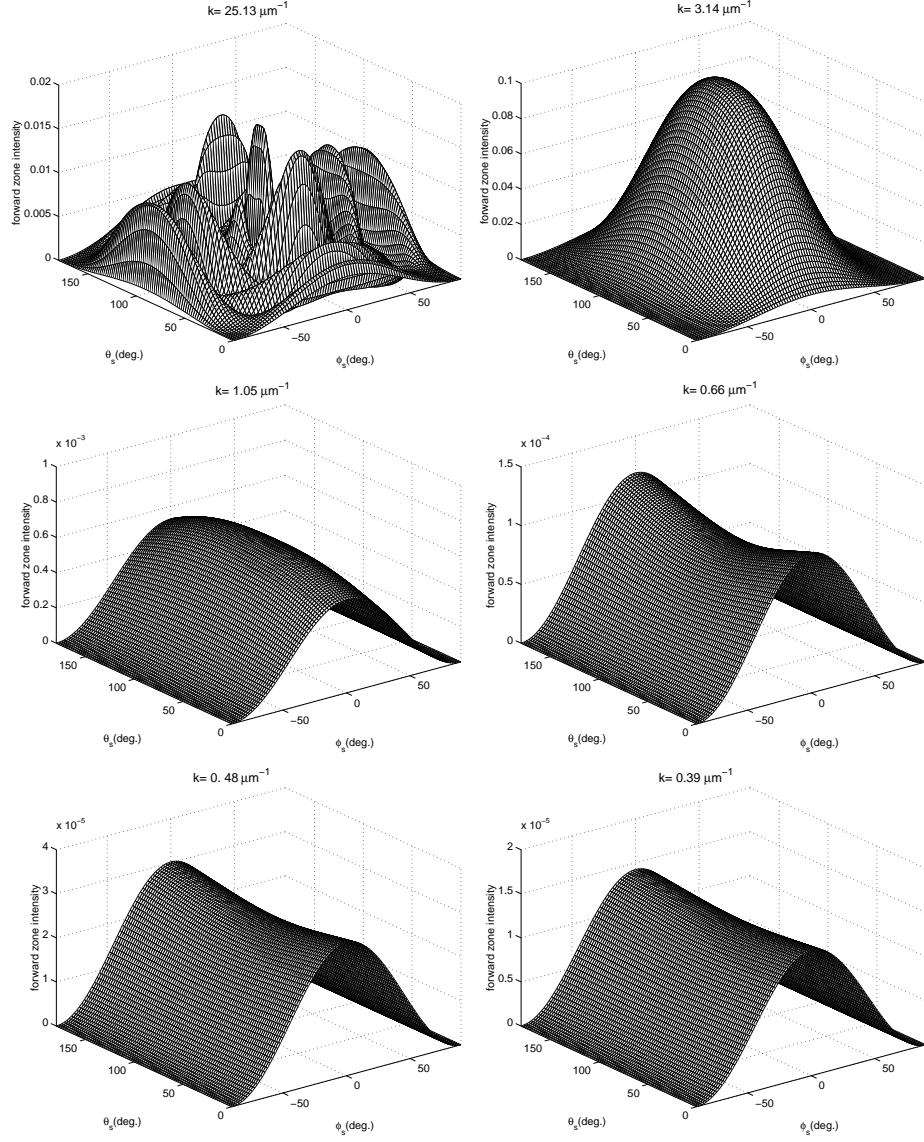
Fig. 5. Scattered intensity in the forward zone for model spores of anthrex in fixed orientation at selected values of the incident wavevector.
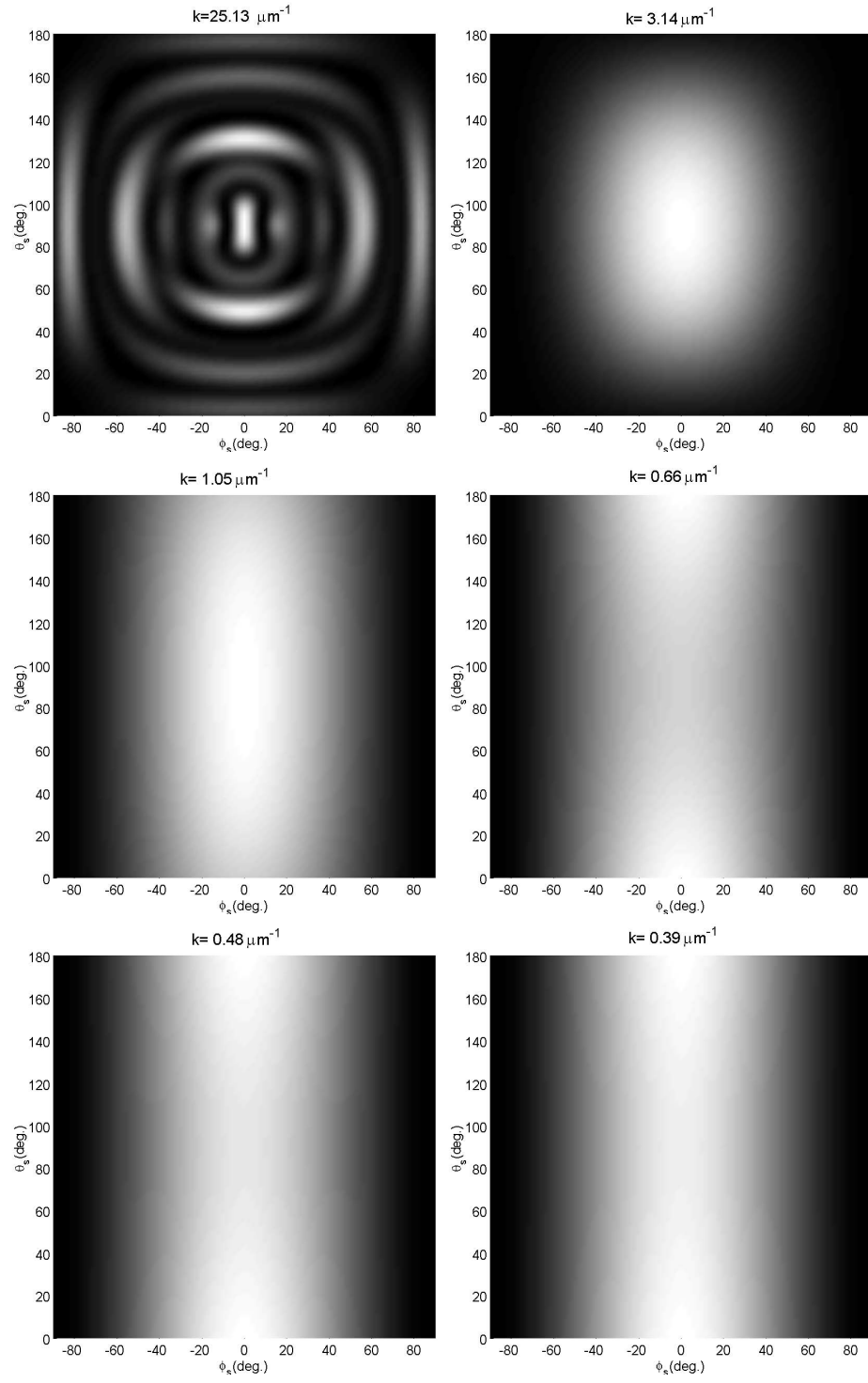
Fig. 6. Contour plots corresponding to the scatterd intensity reported in Fig.(5).

## 3.   Effect of the presence of a nucleus

In the present section we investigate the changes undergone by the optical properties of our model when the component spheres are assumed to have a nucleus or when the radius of the spheres is allowed to change. To this end, when we consider single spores in free space the geometry is that of Fig.3. Note that, in this section the wavevector of the incident field is taken to be parallel to the $z$ axis and that the polarization is either along the $x$ axis (polarization 1) or along the $y$ axis (polarization 2). In order to improve the model we considered the case in which the component spheres, each of radius $r_{\mathrm{s}} = 0.35\,\mu\mathrm{m}$, have a nucleus of comparatively strong absoptivity. To this end we included in each of the component spheres a centered inclusion whose radius is either 80 % or 90 % of the radius of the host sphere. We chose to perform the calculations at $\lambda = 2\,\mu\mathrm{m}$ because at this wavelength the size parameter of each of the host spheres is $x \approx 1$. Since the corresponding dielectric constant
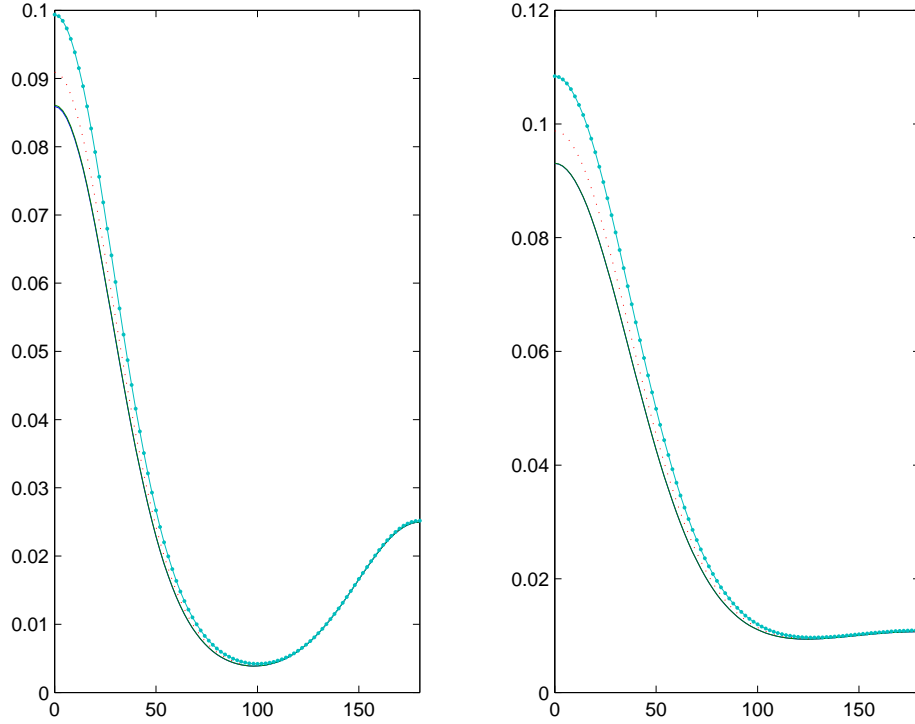


Fig. 7. Scattered intensity $I_{11}$ (a) and average scattered intensity $\bar{I}_{11}$ (b), in $\mu\mathrm{m}^2$, at $\lambda = 2\,\mu\mathrm{m}$ as a function of the angle of scattering $\theta_{\mathrm{S}}$ for the original cluster (solid line) for the cluster with nucleus with radius $r_{\mathrm{N}} = 0.8\,r_{\mathrm{s}}$ (dotted line) and with nucleus with radius $r_{\mathrm{N}} = 0.9\,r_{\mathrm{s}}$ (solid line with bulletts).

is $\varepsilon_0 = 2.23 + i9.89 \cdot 10^{-4}$ we chose for the nucleus the dielectric constant $\varepsilon_1 = 2.5 + i1.09 \cdot 10^{-3}$. The results for the scatterd co-polarized intensity $I_{11}$ as a function of the angle of scattering $\theta_{\mathrm{S}}$ are shown in Fig.7 (a) in case of fixed orientations and in Fig.7 (b) in case of random orientation.

We also made a calculation at $\lambda = 13\,\mu\mathrm{m}$ where the component spheres have a size parameter $x \approx 0.1$ and a dielectric constant $\varepsilon_0 = 2.20 + i7.57 \cdot 10^{-2}$. In this case we assumed for the nucleus a dielectric constant $\varepsilon_1 = 2.4 + i8.5 \cdot 10^{-2}$. The results of our calculations are reported in Fig.8 (a) for the case of fixed orientation and in Fig.8 (b) for the case of random orientation.

Even a cursory examination of Figs.7 and 8 shows that the presence of the nucleus produces
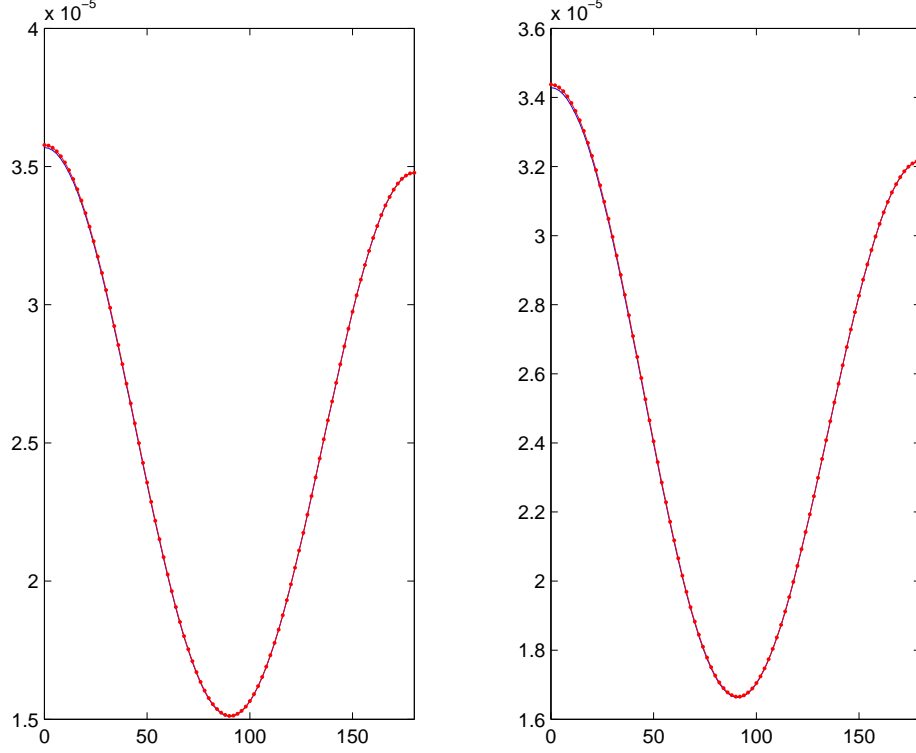
Fig. 8. Scattered intensity $I_{1\,1}$ (a) and average scattered intensity $\bar{I}_{1\,1}$ (b), in $\mu\mathrm{m}^2$, at $\lambda = 13\,\mu\mathrm{m}$ as a function of the angle of scattering $\theta_\mathrm{S}$ for the original cluster (solid line) for the cluster with nucleus with radius $r_\mathrm{N} = 0.8\,r_\mathrm{s}$ (dotted line) and with nucleus with radius $r_\mathrm{N} = 0.9\,r_\mathrm{s}$ (solid line with bulletts).

little difference from the original cluster composed of homogeneous spheres. In particular no change at backscattering is detectable, both for fixed and for random orientation. Moreover, the scattered intensity at $\lambda = 13\,\mu\mathrm{m}$, shows, as expected a strong decrese, that may be compensated only in case the observations are made on a dispersion containing a high number of spores.

## 4. Dependence on size

The geometry that has been adopted until now is based on the estimate of the actual size of the spores made on the basis of electron microscopy. Of course these estimates are affected by the experimental uncertainties. Therefore in the present section we compare the extinction cross sections of model spores modeled as aggregates of two identical spheres whose radius is allowed to change within the limits of the experimental uncertainties. The spectrum has been calculated in the wavelength range $0.1 \leq \lambda \leq 8.0\,\mu\mathrm{m}$ where the differences induced by the change of size are easily discernible. In Fig.9 we report the extinction cross section, averaged for random orientation, for several values of the radius of the component spheres. We also report, for the sake of comparison the extinction cross section of the volume equivalent sphere, whose radius, according to the laboratory data, is $r_\mathrm{e} = 0.6306\,\mu\mathrm{m}$. In Fig.10 we report the extinction cross section for clusters in fixed orientation (according to Fig.3) when the field is polarized along the $x$ axis. A look to Fig.9 shows that, with increasing radius of the component spheres, the main extinction peak tends to shift towards higher
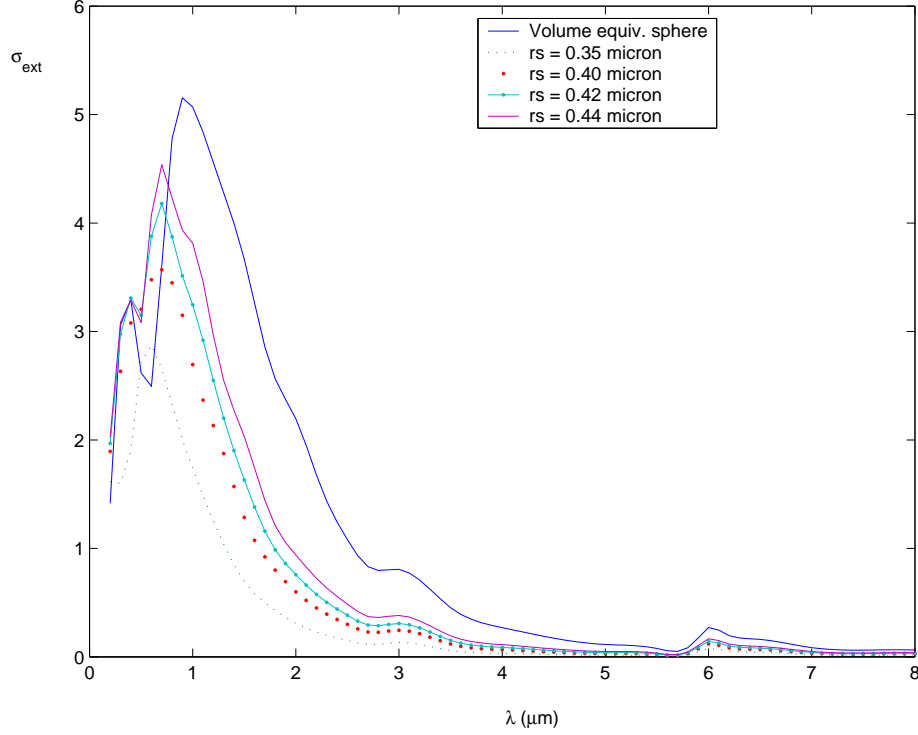
Fig. 9. Extinction cross section in $\mu$m$^2$ averaged for random orientation as a function of the wavelength for the original cluster and for three further choices of the radius of the component spheres. The cross section of the equivalent volume sphere of radius $r_e = 0.6306\,\mu$m is also reported for the sake of comparison.

wavelengths so as to superpose to the main peak of the volume equivalent sphere. Nevertheless the superposition never occurs in the range of radii that we consider here. The same is true for the case of fixed orientation, as can be seen in Fig.10. We found that the behavior displaied in Fig.10 also pertain to the curves for fixed orientation and polarization along the $y$ axis: a specific figure is therefore not reported.

In conclusion we can state that, the behavior of the model has little dependence on the presence of a nucleus but that it may, even appreciably, depend on the size of the spheres that are used to build the model. Further investigation on this point is still in progress. We also plan to consider the scattering pattern from our model spores deposited on a plane surface. Note that we are able to perform the latter task both in case of a dielectric and of a metallic surface.[1]

## 5.  Scattering from rehydrated spores

In the preceding reports we stressed that the main problem with the individuation of the spores of anthrax and of any other bacteriological agent lies not so much in determining the exact form and size of the single spores, as in determining their "exact" refractive index. In fact, all our calculations suggest that the possibility of finding some feature of the optical spectra of biological spores that permits the discrimination of a particular type, do depend on the exact knowledge of the refractive index. For this reason, in the last few months we focused on checking the results of the most recent papers whose aim was the measure of the refractive index of single spores. In the present report
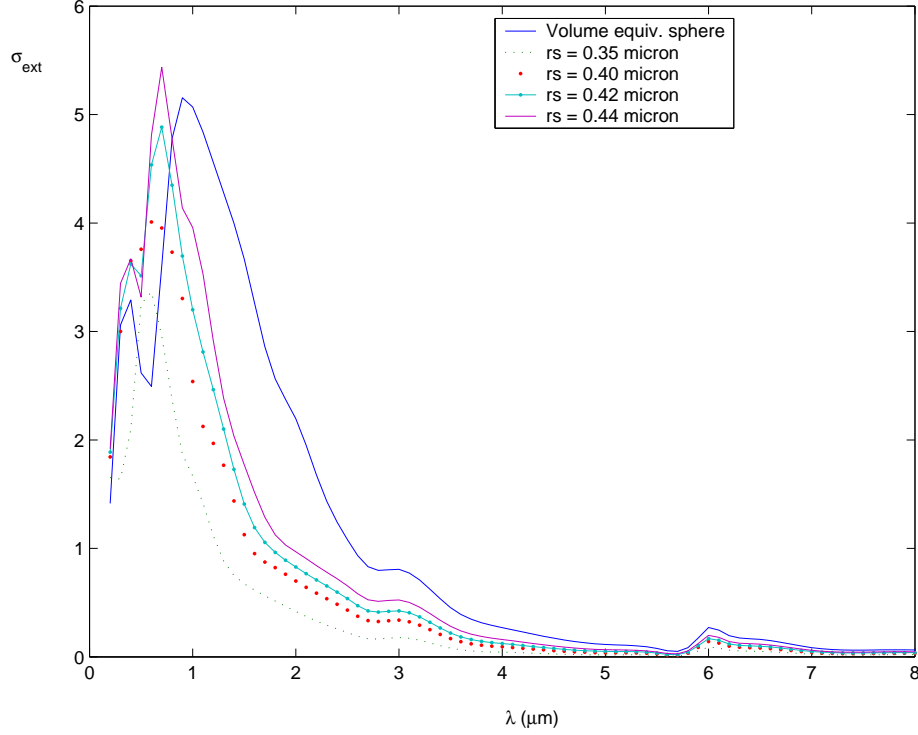
Fig. 10. Same as Fig.9 but for clusters in fixed orientation and broadside incidence. The incident electric field is polarized along the $x$ axis

we describe our check of the results reported in the paper: A.Katz, A.Alimova, M.Xu, P.Gottlieb, E.Rudolph, J.C.Steiner, R.R.Alfano In situ determination of refractive index an size of Bacillus spores by light transmission Optics Letters 30, 589-591, 2005. In this respect let us stress that B. Subtilis is considered by many workers the best simulant of the spores of anthrax. In summary, the authors calculated the scattering power of single spores of B. Subtilis in the wavelength range 400-1000 nm; in this range the absorption from the single spores is negligible so that the refractive index can be considered to be real. Dry spores are put into a nourishing solution and the scattering from a test tube filled with the resulting dispersion is measured under controlled laboratory conditions. The dry spores turn out to be composed by a mantle whose refractive index is smaller than that of the core, but, when immersed into the nourishing solution, activate and lose their mantle within two hours. After six hours the activation process is complete and the spores shows a fully hydrated core and becomes nearly vegetative. The authors assume that, under these conditions, the "anomalous diffraction approximation" is valid, so that the scattering cross section is given by

where the coefficients c1 and c2 depend on the size parameter and on the refractive index of the scattering object. From the best fit of the optical attenuation one gets the numerical estimate of the coefficients c1 and c2 as a function of the time during which the spores lie immersed in the nuorishing solution. The evaluation of the size parameter and the refractive index of the spores require the choice of a suitable model. The authors choose two models: 1) Homogeneous, non-layered spheres; 2) Spherical layered spheres

In the first case the experimental data yield: Initial radius of the dry spore: 0.35 micron Final radius (after 6 hours) : 0.6 micron Initial refractive index : 1.55 micron (this value overestimates the
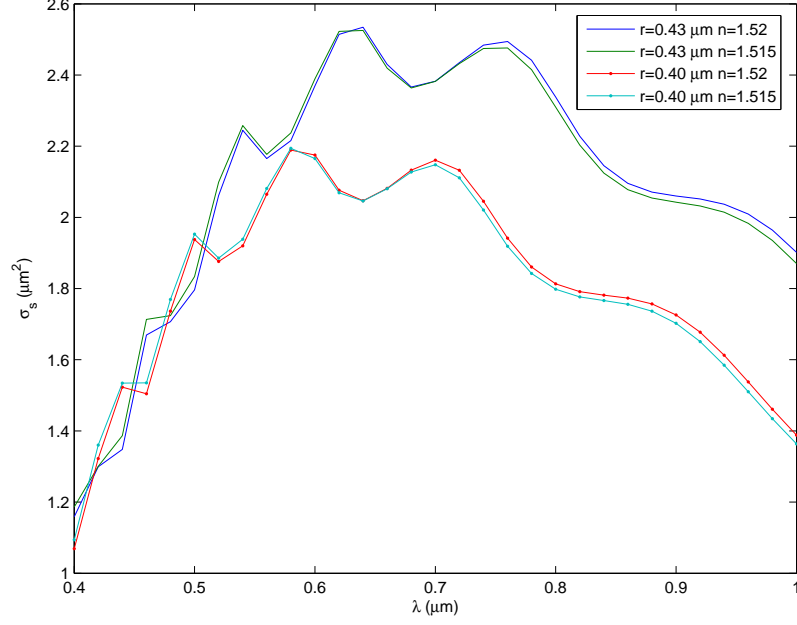
Fig. 11. ...

reference value derived by Tuminello) Refractive index after 3h (this is the time required to allow the spore to lose its mantle): 1.39

In the second case one assumes that initially the spore is simulated by a sphere of 0.4 micron inclusive of a coating of 0.070 micron and refractive index 1.39. The refractive index of the coating decreases linearly as a function of time and becomes 1 within 3h; the refractive index of the core is assumed to be 1.55. Under these assumptions, the experimental data yield:

Initial radius of the dry spore : 0.38 $\mu$m Final radius (after 6 hours) : 0.6 $\mu$m Initial refractive index : 1.52 $\mu$m (this value is nearly equal to the one derived by Tuminello n=1.515) Refractive index after 3h (this is the time required to allow the spore to lose its mantle): 1.39

The choice of the initial parameters has been made by the authors on the consideration that the dry spores when observed through a microscope show an ellipsoidal shape whose axes are 1.25 micron and 0.75 $\mu$m. These spores produce the same attenuation of a sphere with radius 0.43 $\mu$m (this value is nearly equal to the chosen for the layered sphere).

At this stage let us describe the work done by our group.

Influence of the refractive index. In order to see to what extent the choice of the refractive index affects the scattering cross section we considered sphere of two typical sizes, according to the suggestion of the authors, namely 0.43 and 0.40 micron. The cross sections were calculated for spheres with refractive index n=1.515 and n=1.52 in the spectral range 400 to 1000 nanometers (See Fig. 11)

Even a cursory examination of Fig. 11 shows that for spheres of equal size varying the refractive index has practically no effect on the general shape of the curves of the scattering cross section as a function of the wavelength. This is an expected result because a variation of 0.3 % in the value of the refractive index cannot introduce detectable changes, especially from the experimental point of view. The preceding considerations, that are based on exact numerical results, are in contrast to the claimed ability of the experimental method and of the method of data elaboration which,
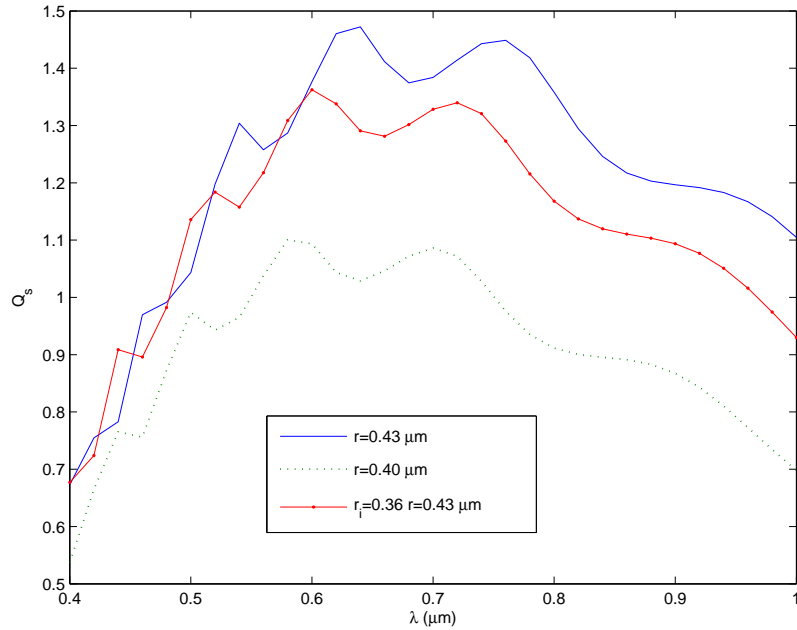
Fig. 12. ...

according to the authors, is capable to attribute to the spores a refractive index n=1.515 (reference value) rather than n=1.52. Closer examination of Fig. 1 shows that the choice of the size has, on the contrary, striking effects. In fact, a change in size of 7 % (from 0.40 to 0.43 $\mu$m) produces a change of the scattering cross section up to 35 %. Note that so strong an effect has never been observed in the results of our exact calculations for non-spherical model spores.

**Effect of the mantle.** Since the dry spores are composed of an optically dense core surrounded by a mantle of lower optical density, we resolved to simulate the scattering properties af the actual objects by a stratified sphere whose nucleus has a refractive index n=1.515 whereas the refractive index of the mantle has been chosen to be n=1.39.

In Fig. 12 we report the scattering efficiency for a layered sphere of total radius 0.43 $\mu$m inclusive of a mantle of 0.07 $\mu$m as well as the scattering efficiency of homogeneous spheres with radius 0.43 and 0.40 $\mu$m. We notice that the presence of the mantle produces a diminution of the scattering efficiency, whose values turn out to be between the values for the bare spheres.

In Fig. 13 we show that the fit obtained by the authors, by considering only the first term (the one in (-2 ), differs from the one obtained by exact calculations for spheres of varying radii.

In conclusion, the comparison of the results reported by the authors with those obtained by our group on the basis of their experimental data, suggest that the size parameter of the spores is too small to grant the applicability of the anomalous diffraction approximation to the interpretation of the experimental results. Furthermore, our results confirm that attempting the interpretation of the experimental data using as a reference spherical models is bound to yield misleading conclusions.

## 6.   Spores on a surface

It is a common laboratory practice to measure the optical properties of small particles after deposition on a dielectric substrate, i.e on a substrate whose conductivity is finite. Of course, since the electromagnetic field may propagate within the substrate, the presence of the latter on the measured
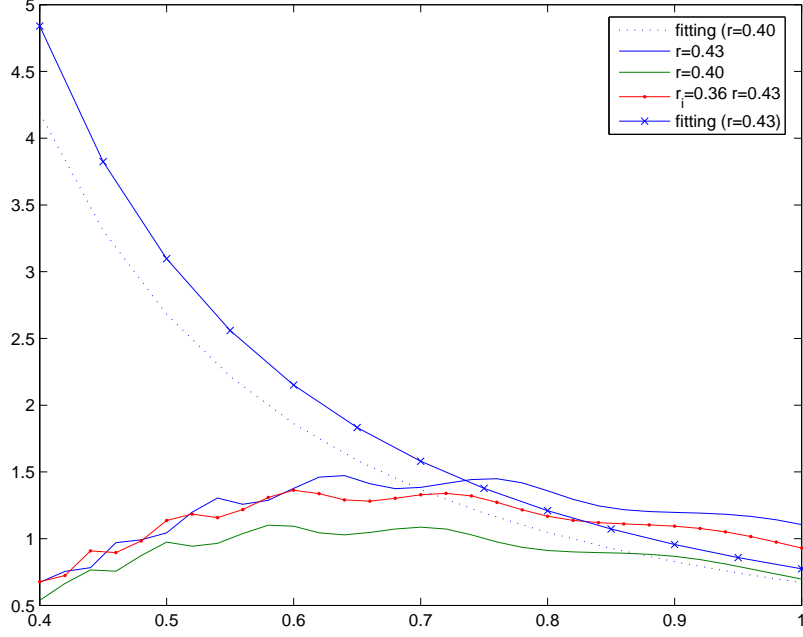
Fig. 13. ...

optical properties of the particles should be carefully discriminated. In fact, the optical properties of the particles that form an aerosol may appear quite different from those of the same particles when deposited on a dielectric surface. On the other hand, many of the surfaces on which an aerosol can deposit have dielectric refractive index. For this reason we calculated the pattern of the scatterd intensity from model spores of anthrax deposited on a substrate of silicon, that is commonly used in laboratory practice.

In order to describe the scattering process from a particle on a surface one has to consider, besides the incident $\mathbf{E}_I$ and the reflected $\mathbf{E}_R$ field also the field scattered by the particle $\mathbf{E}_S$ as well as the field that after scattering by the particle is reflected by the surface $\mathbf{E}_{SR}$. Now, the field scattered by any particle can be expanded in a series of spherical vector multipole fields that satisfy the radiation condition at infinity. Therefore, it is essential, in order to calculate $\mathbf{E}_{SR}$, to have a rule for the reflection of the spherical multipole fields on a plane surface. To this end we used the procedure based on the Multipole Reflection Theory (MRT) that our group devised in 1997.[1,3] In practice MRT solves the problem of reflection of a spherical multipole satisfying the radiation condition at infinity on a plane surface whose (possibly complex) refractive index is finite. Note that the scattered field is to be considered in the near zone, so that no simplifying approximation applies. For instance, the approximations devised by Johnson and by Bobbert and Vlieger[5] have the undesirable consequence of preventing the propagation of the field within the dielectric material of the substrate. On the contrary, what distinguishes the results of our approach from those of other workers in the field is the presence of a field that propagates along the interface, according to the boundary conditions to the Maxwell equations. Anyway, our approach grants a smooth transition to the case in which the interface is metallic and thus has, by definition, an infinite imaginary part of its refractive index.

It is to be mentioned that using the MRT requires a careful check of the convergence. Extensive test calculations have in fact shown that using MRT implies a rate of convergence that grows slower the higher the imaginary part of the refractive index.[4]

A further aspect of our approach is the possibility of defining the transition matrix for the particles on the surface. This possibility is quite useful because the transition matrix possess well defined transformation properties under rotation of the coordinate frame. As a result, it becomes an easy matter to perform averages over the orientational distribution of the particles.[1]

## 7.  Reference frame

It is usual to perform the calculations for the scattering pattern from particles deposited on a surface by assuming a frame of reference whose z axis is orthogonal to the surface. Also the theory is based on this choice of the frame of reference, that is hardly compulsory, however. In fact, in order to display the results of our calculations we preferred to choose a different frame of reference that is better described in Fig.14. Accordingly the dielectric surface is chosen to coincide with the zx plane and the normal is therefore coincident with the y axis.
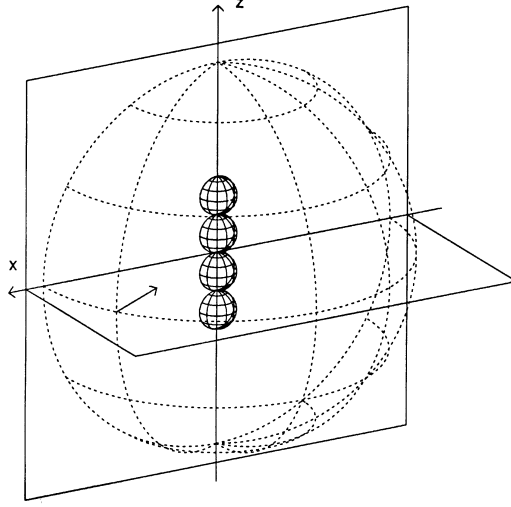


Fig. 14. Frame of reference that has been chosen to display the results of our calculations. The arrow on the equatorial plane indicates the direction of incidence, that forms an angle of 45° with the normal to the surface.

Accordingly, the range of the polar angles of the direction of observation are $0 \leq \vartheta_S \leq \pi$ and $0 \leq \varphi_S \leq 2\pi$. In Fig.14 the direction of incidence is indicated by an arrow and its polar angles are $\vartheta_I = 225°$ and $\varphi_I = 45°$; in other word we chose the direction of incidence to form an angle of 45° with the normal to the surface. This defines the plane of incidence as the xy plane. The polarization of the incident and of the scattered field has been fully taken into account. In fact we considere the incident field polarized both along the meridians ($\vartheta$-polarization) and along the parallels ($\varphi$-polarization) and the components of the scattered field both $\vartheta$-polarized and $\varphi$-polarized are considered. Therefore, in the following figures we display the scattered intensities generated by an incident field with both kinds of polarization. In this respect we stress that the presence of the surface implies the occurrence of cross-polarization effects even when the actual particle is a single sphere. In all cases, due to the generality of our approach we are able to report the full scattering pattern, i.e. our results are not restricted to the plane of incidence.
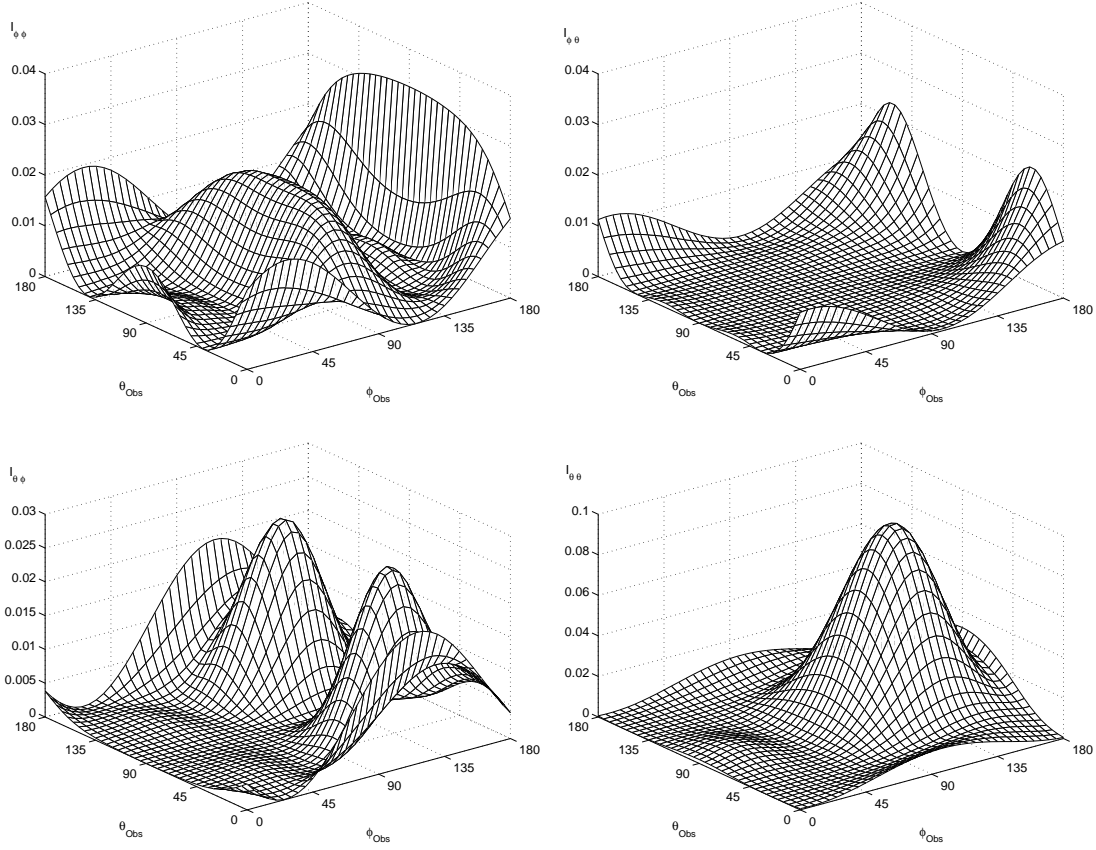
Fig. 15. Pattern of the scattered intensity from spores of anthrax with their axis along the x axis. The quantity that we actually report, in $\mu m^2$, is $\mathcal{I}_{\eta\eta'} = r^2 I_{\eta\eta'}/I_0$.

## 8.  Results

For the calculations that are described below, we assumed a refractive index for the dielectric material to be $n'' = 1.3$ that is appropriate for silicon in the visible and the near infrared. The choice of a real refractive index is in no way a limitation, its only effect being to increase the rate of convergence; of course, nothing prevents the calculation on a surface whose refrative index is complex. As usual the spores of anthrax are modeled as a cluster of two identical spheres of radius $\rho = 0.35\,\mu m$ . The refractive index of the spheres is assumed to be identical to that of the B. Cereus for reasons that were fully explained in our preceding reports. The wavelength of the incident radiation is $\lambda = 2.0\,\mu m$ and the direction of incidence is characterized by the polar angles $\vartheta_I = 90°$ and $\varphi_I = 225°$, i. e. the direction of incidence forms an angle of 45° with the normal to the surface. Note that in order to perform our calculations we assume that the spores form a monolayer on the surface and that their density is so small that multiple scattering processes are negligible. According to Reichl[6] if multiple scattering processes were to be considered, the pattern of the scattered intensity would contain terms that describe the positional correlation of the particles.

In Fig. 15 we report the pattern of the scattered intensity for equioriented spores with their axis along the $x$ axis (see Fig. 14). As usual we do not include the intensity of the reflected field because the latter would be detectable only along the direction of reflection In Fig. 16 we report the
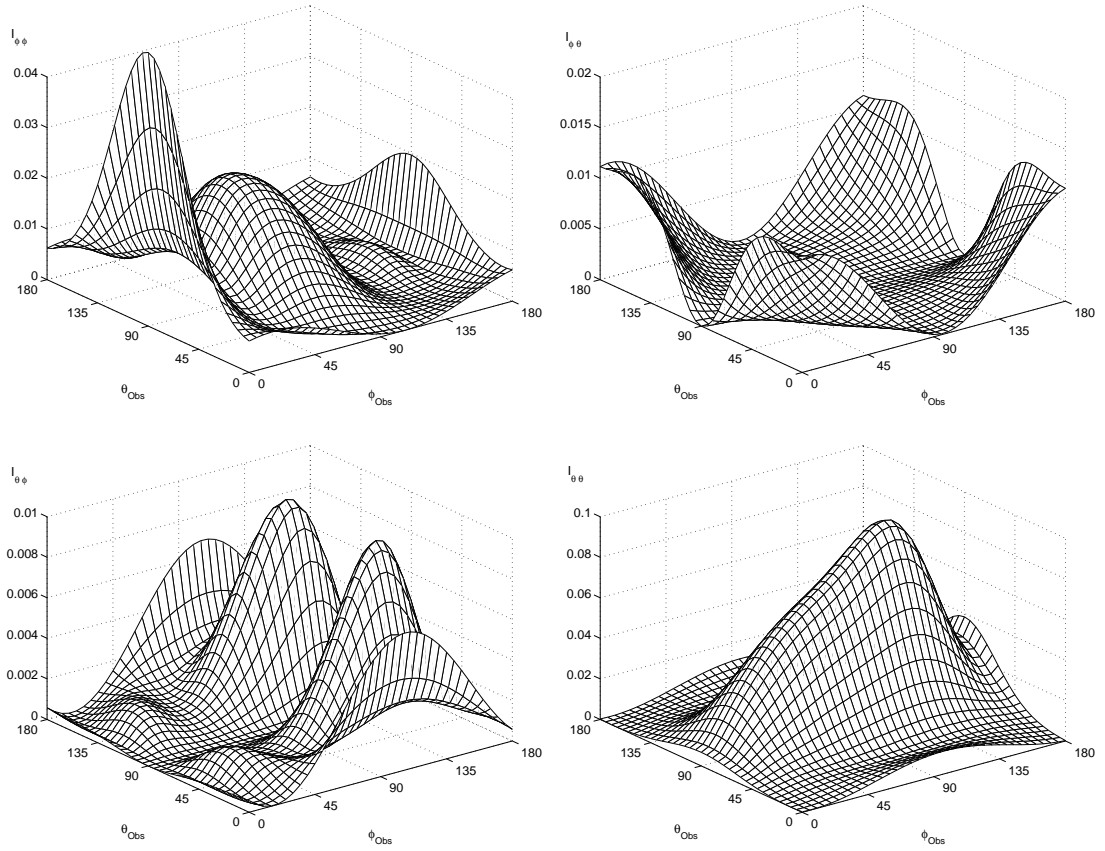
Fig. 16. Pattern of the scattered intensity from spores of anthrax with their axis along the z axis. The quantity that we actually report, in $\mu m^2$, is $\mathcal{I}_{\eta\eta'} = r^2 I_{\eta\eta'}/I_0$.
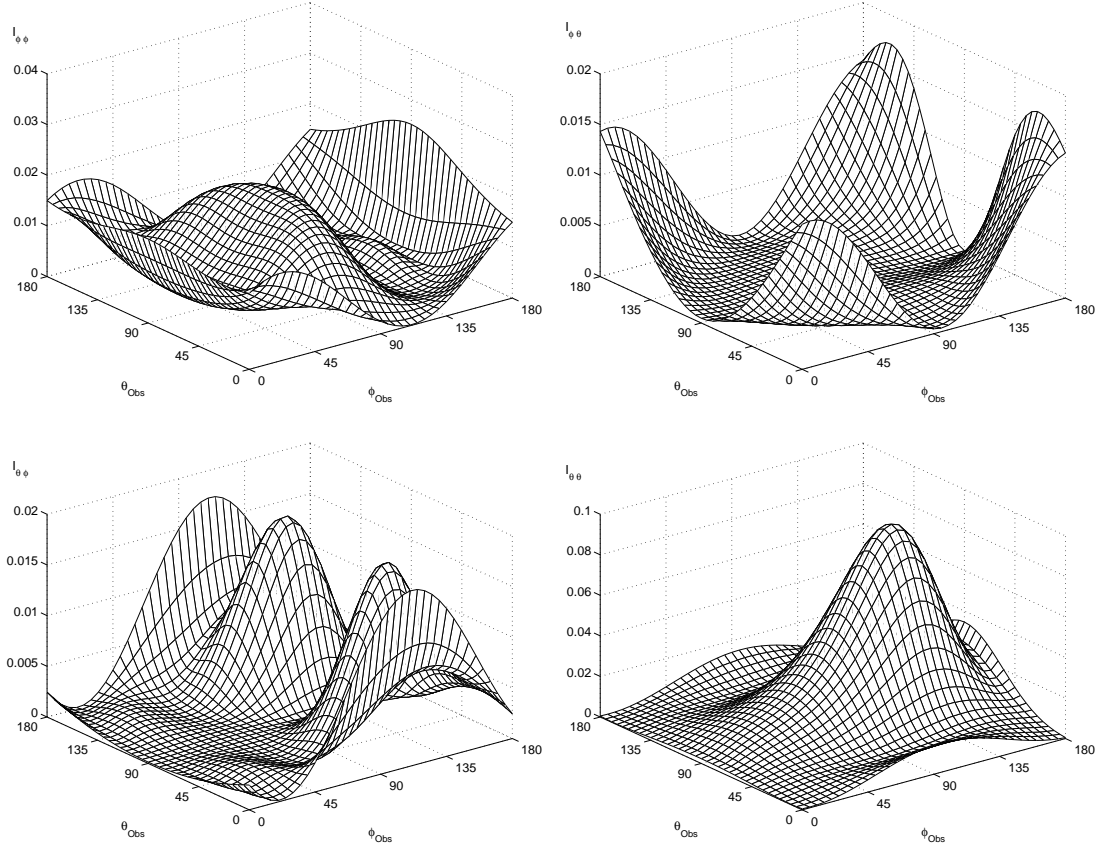
16

Fig. 17. Pattern of the scattered intensity from a random orientational distribution of model spores of anthrax. The quantity that is actually reported is $r^2 \langle I_{\eta\eta'} \rangle / I_0$ in $\mu m^2$, where the angular brackets denote random orientational average.

same kind of pattern but for the axis of the spores along the $z$ axis, i. e. for broadside incidence.

Finally, we report in Fig. 17 the pattern from spores on the surface, averaged over a random orientational distribution. In fact, it is rather unlikely that spores deposited on a surface assume a definite orientation.

## References

1. F. Borghese, P. Denti and R. Saija, *Scattering from model nonspherical particles*, (Springer, Heidelberg, 2002)

2. A.Katz, A.Alimova, M.Xu, P.Gottlieb, E.Rudolph, J.C.Steiner, R.R.Alfano, "In situ determination of refractive index an size of Bacillus spores by light transmission," Optics Letters 30, 589-591, 2005

3. E. Fucile, F. Borghese, P. Denti, R. Saija and O. I. Sindoni, "General reflection rule for electromagnetic multipole fields on a plane interface," IEEE Trans. Antennas Propag. **AP 45**, 868–875 (1997).

4. E. Fucile, P. Denti, F. Borghese, R. Saija and O. I. Sindoni, "Optical properties of a sphere in the vicinity of a plane surface," J. Opt. Soc. Am. A **14**, 1505–1514 (1997).

5. P. A. Bobbert and J. Vlieger, "Light scattering by a sphere on a substrate", Physica **137 A**, 209–242 (1986).

6. L. E. Reichl, *A modern course in statistical physics*, (University of Texas Press, Austin, 1980).